Metal–Organic Frameworks

DOI: 10.1002/anie.201104240

Enantiopure Metal–Organic Framework Thin Films: Oriented SURMOF Growth and Enantioselective Adsorption**

Bo Liu, Osama Shekhah, Hasan K. Arslan, Jinxuan Liu, Christof Wöll, and Roland A. Fischer**

Growing effort is being paid to metal–organic frameworks (MOFs), in the form of microcrystalline powder materials, for the storage, capture and separation of gases and for applications in catalysis.[1] The demand of integrating MOFs into analytical sensing devices and smart membranes is stimulating the development of MOF thin-film possessing techniques of various kinds.[2] In this respect, the layer-by-layer (LBL) liquid-phase epitaxial (LPE) growth method is quite attractive for depositing multilayers or small crystallites of surface-attached MOFs (SURMOFs) in an automatic and thus very controlled fashion.[3] This stepwise MOF synthesis and deposition scheme can be coupled with in-situ process monitoring by UV/Vis spectroscopy, surface plasmon resonance spectroscopy (SPR), or by quartz crystal microbalance techniques (QCM) and provides unique opportunities to study the (SUR)MOF growth mechanism[4] and is advantageous for MOF-based sensor fabrication.[5] LPE is also well suited for deposition of MOF (hetero-)structures,[6] for suppressing interpenetration,[7] and for tailoring the chemical functionality of the external SURMOF surface,[8] tasks which are quite difficult to achieve for MOF thin films grown by other deposition techniques. In particular SURMOFs of HKUST-1 allow the monitoring of adsorption/desorption of guest molecules at ultra thin and very homogeneous coatings and allow the determination of the corresponding diffusion constants.[9] Using these concepts we now demonstrate LPE growth of $[\{Zn_2((+)cam)_2(dabco)\}_n]$ ((+)cam = (1*R*,3*S*)-(+)-camphoric acid, dabco = 1,4-diazabicyclo(2.2.2)octane)) and the application of this very first example of an enantiopure SURMOF to the direct QCM monitoring of the uptake of a pair of enantiomeric guest molecules, namely (2*R*,5*R*)-2,5-hexanediol (R-HDO) and (2*S*,5*S*)-2,5-hexanediol (S-HDO) from the gas phase under flow conditions.

[*] Dr. B. Liu, Prof. Dr. R. A. Fischer
Chair of Inorganic Chemistry II—
Organometallics and Materials Chemistry
Ruhr-Universität Bochum, 44870 Bochum (Germany)
E-mail: roland.fischer@rub.de

Dr. O. Shekhah, H. K. Arslan, Dr. J. Liu, Prof. Dr. C. Wöll
Institute of Functional Interfaces (IFG)
Karlsruhe Institute of Technology (KIT)
76344 Karlsruhe (Germany)
E-mail: christof.woell@kit.edu

[**] This work was funded within the priority program of the German Research Foundation (DFG) on Metal–Organic Frameworks (SPP 1362). B.L. is grateful for a stipend from the Alexander von Humboldt Foundation. SURMOFs = surface-mounted metal–organic frameworks.

Supporting information for this article is available on the WWW under http://dx.doi.org/10.1002/anie.201104240.

Microcrystalline MOF powder materials have been explored as stationary phases in both gas[10] and liquid-phase chromatography[11] and related theoretical and experimental studies on the diffusion in MOF single crystals have been reported.[12,13] Quite recently, the LBL growth scheme was adopted for coating fused silica capillaries with MOF-5 for the first time.[14] Accordingly, enantiopure MOFs are highly promising for the separation of enantiomers, a result of their high porosity, functional diversity, flexibility, and size and shape selectivity, surpassing other porous materials.[1,10] The technological challenge is to achieve LPE growth of enantiopure SURMOFs as a model to study in detail enantioselective adsorptions on well-defined MOF coatings.

Multicomponent layer-based MOFs of the general formula $[\{M_2L_2P\}_n]$ (M: Cu^{2+}, Zn^{2+}; L: dicarboxylate linker; P: dinitrogen pillar ligand)[15] have been shown to be favorable for step-by-step LPE.[6] Our test case, $[\{Zn_2(cam)_2(dabco)\}_n]$ (+)-**1** for (+)cam and (−)-**1** for (−)cam) with an anisotropic tetragonal crystal system is such a layer-based MOF containing the binuclear "paddle wheel" zinc carboxylate unit $\{Zn_2(COO)_4N_2\}$ with distorted octahedral geometry, in which chiral camphorate bridge the dimeric zinc units into infinite planar layers $\{Zn_2cam_2\}_n$. Linear N-donor ligands dabco occupy the axial Zn sites, perpendicularly to these $\{Zn_2cam_2\}_n$ layers, leading to a scaffold-like 3D structure.[16] The structure allows two principle growth directions depending on carboxylate and pyridine groups location (Figure 1). Typically, the enantiopure SURMOFs (+)-**1** or (−)-**1** are grown (20–40 cycles) by dipping the QCM substrate alternately in ethanol solutions of $Zn(Ac)_2{\cdot}H_2O$ and equimolar (±)cam/dabco mixtures, each step followed by immediately rinsing with pure ethanol, according to the procedure developed in our group (Figure 1).[6] The growth process was monitored in situ by QCM as shown in Figure S1 in the Supporting Information. The crystallite orientation of the samples can be controlled by applying self-assembled monolayer (SAM) modified QCM substrates with different functional head groups (pyridyl or carboxylate) and appropriate growth conditions.[6]

As examined by surface X-ray diffraction in an out of plane mode (Figure 2), SURMOF (+)-**1** was grown in (110) and (001) orientation on SAMs of MHDA and PPMT (MHDA = 16-mercaptohexadecanoic acid; PPMT = (4,(4-pyridyl)phenyl)methanethiol)) on Au-coated QCM substrates. The (110) and (001) X-ray diffraction (XRD) peak positions are very close to each other at 9.28° and 9.22° which is in accord with the corresponding single-crystal X-ray diffraction data.[16] To accurately distinguish these two peaks, the XRD peak positions were calibrated by referencing to the XRD peak positions of the Au substrate. Accordingly,

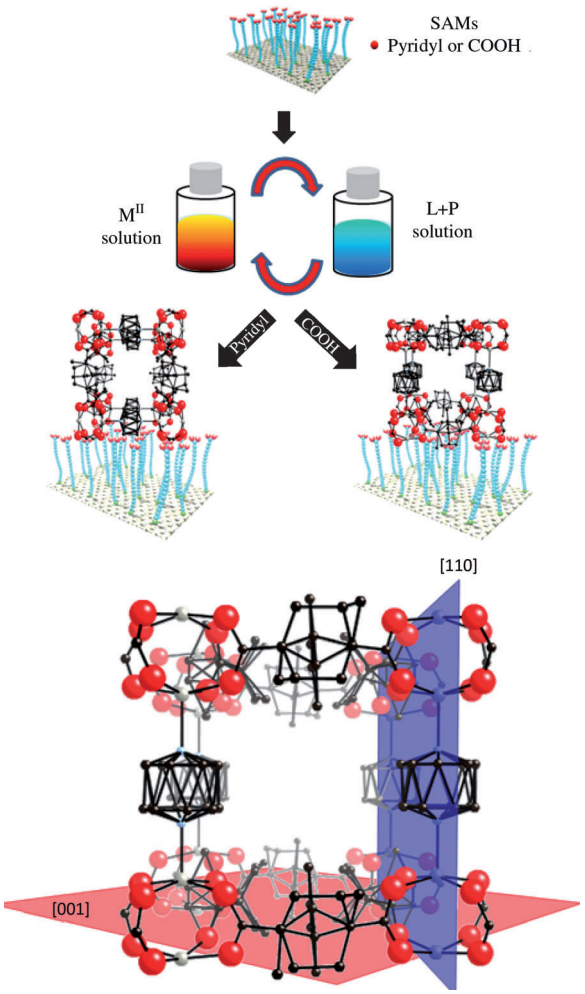

Figure 1. Top: Two principle growth directions and of $[\{Zn_2(cam)_2(dabco)\}_n]$; bottom: schematic illustrations of oriented growth in the (001) orientation on pyridyl-terminated (PPMT) and the (110) orientation on COOH-terminated (MHDA) SAMs on gold substrates. See the Supporting Information for further details.

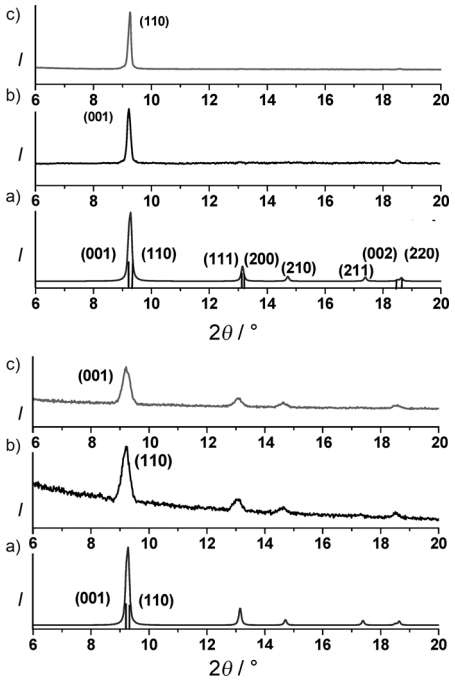

Figure 2. Comparison of XRD patterns of SURMOF (+)-**1** with reference data a) simulated from single-crystal XRD data of $[\{Zn_2((+)cam)_2(dabco)\}_n]$.[16] Top: Out-of-plane XRD patterns of (+)-**1** grown in b) the (001) orientation on PPMT SAM/Au and c) in the (110) orientation on MHDA SAM/Au. Bottom: In-plane XRD patterns of (+)-**1** grown on PPMT SAM/Au in b) the (001) and c) in the (110) orientation on MHDA SAM/Au. All the samples are LPE grown on QCM substrate (40 cycles).

the (220) and (002) diffraction peaks can be distinguished clearly. In-plane XRD patterns for SURMOFs (+)-**1** in both orientations perfectly match with the simulated patterns from single-crystal XRD (Figure 2). To confirm the reproducibility and orientation assignments perpendicular to the substrate surface, out-of-plane XRD measurements are carried out independently on another two pairs of samples which gave the same results (Figure S2 and S3 in the Supporting information). IR spectra of the SURMOFs (+)-**1** in the two orientations display no difference (Supporting Information, Figure S4). Similarly, we also prepared the enantiomeric SURMOF (−)-**1** in (110) orientation on a MHDA SAM, as characterized by XRD (Supporting Information, Figure S5). As expected, the data is identical to that for (+)-**1**.

The ability of SAMs containing functional groups to control nucleation of crystal growth has been well established,[17] and the templating role of SAMs towards SURMOF orientation has been addressed in detail.[3–9] Once exposed to $Zn(Ac)_2{\cdot}H_2O$, carboxylate groups on the MHDA SAM will fix the paddle-wheel structured zinc dimer on the surface by replacing acetate groups from equatorial plane, which regulates SURMOF growth in the (110) orientation. Subsequent deposition of a mixture of (+)cam/dabco leads to occupation of axial sites by dabco and equatorial plane sites by (+)cam. In contrast, on the PPMT SAM the pyridine group will coordinate to the axial sites of the zinc dimer, and thus induce growth along the (001) orientation.

The quartz crystal microbalance (QCM) is an ultrasensitive device capable of sensing mass changes in the nanogram range. The deposition of enantiopure SURMOFs (+)-**1** and (−)-**1** directly on the QCM substrate enables the adsorption kinetics of enantiomeric probe molecules to be monitored by QCM and thus allow assessing the adsorption enantioselectivity of the MOF thin film. Since the layers $\{Zn_2cam_2\}_n$ are quite dense and inaccessible for incoming molecules, the available entrance only exists in the space between the layers strutted by pillar linker of dabco for both (110) and (001) orientated samples (Figure 1). We selected SURMOFs (+)-**1** and (−)-**1** in (110) orientation to study the adsorption of R- and S-HDO from the gas phase (vapor) in a continuous-flow mode using nitrogen gas as carrier. The particular probe molecule 2,5-hexandiol (HDO) was chosen because its dimensions complement the pore sizes and the possibility of H-bonding with the Zn-carboxylate groups of the framework.[18]

Table 1 shows the saturated adsorption value (at 800 min of exposure) of R- and S-HDO over SURMOFS (+)-**1** and

Table 1: Specific mass uptake ($\mu g\,cm^{-2}$) from the gas phase of the enantiomeric probe molecules R- and S-HDO over (110) oriented SURMOFs (+)-**1** and (−)-**1**.[a]

	(+)-**1**	(−)-**1**
R-HDO	0.388	0.211
S-HDO	0.254	0.321
Enantioselectivity[b]	1.55 (0.64)[c]	0.66 (1.52)[c]

[a] Saturated adsorption value. [b] Enantioselectivity is qualitatively denoted as the ratio of saturated adsorption values (at 800 min of exposure) of R-HDO/S-HDO. [c] Ratio of S-HDO/R-HDO.

(−)-**1**. The results indicate that (+)-**1** displays a roughly 1.5-fold preference for adsorption of R-HDO over S-HDO, whereas (−)-**1** exhibits the inverted selectivity, a 1.5-fold adsorption of S-HDO over R-HDO. This very significant difference is attributed to the different interaction of R- and S-HDO with SURMOF containing (+) and (−) forms of camphorate. QCM adsorption profiles are presented in Figure 3. In contrast, the enantioselectivity of adsorption of R/S-HDO by an amino acid-based enantiopure MOF, used as polycrystalline powder material, is very low ($[Ni_2(l\text{-asp})_2(bipy)]$, asp: aspartic acid, bipy: 4,4′-bipyridine).[18]

Before each adsorption experiment, the respective SURMOF sample was activated (vacuum treatment at room temperature) to remove ethanol molecules (solvent) hosted in the framework (checked by FTIR). The sample was purged with high purity nitrogen to obtain a stable QCM baseline. Afterwards, the nitrogen carrier gas was switched to the vessel containing hexanediol to allow vapor of HDO to flow over the SURMOF sample at room temperature. The adsorption/desorption process was monitored by QCM (Supporting Information, Figure S6). Adsorption rates after 200 min (reflected by the slope of the adsorption curve) are almost the same for both experiments, as displayed in Figure 3. However, the adsorption rates at the first 60 min are distinct for R- and S-HDO over (+)-**1** and (−)-**1**, respectively (Supporting Information, Figure S7 and S8). This different adsorption rate is vital for enantioselective separations. From these experiments, we can conclude that SURMOFs (+)-**1** and (−)-**1** behave as enantiopure thin films to separate R- and S-HDO based on both adsorption rate and saturation amount for each enantiomer. Infrared reflection absorption spectroscopy (IRRAS) was used to confirm the adsorption of HDO (Supporting Information, Figure S9). In comparison with blank SURMOF samples, a broad band cantered at 3468.4 cm^{-1} appeared after adsorption, which corresponds to the hydrogen bonds of HDO molecules adsorbed in the framework. This hydrogen-bond interaction may contribute to the interaction of the HDO with the framework, as HDO is strongly adsorbed and difficult to remove by purging with pure nitrogen gas at ambient conditions (Supporting Information, Figure S6). However, the peak characteristic of HDO disappears completely on vacuum treatment. Over the same sample, adsorption of the other enantiomer of HDO was measured to avoid any errors generated from using different samples (and this switching between the enantiomers was repeated several times).

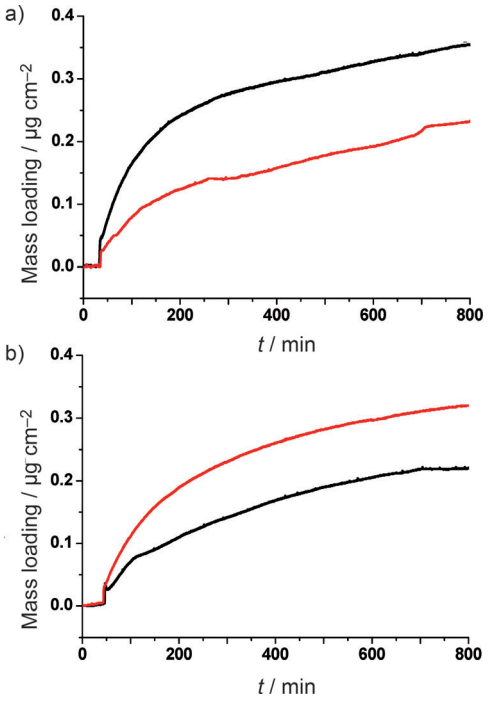

Figure 3. QCM profiles of specific mass uptake of each enantiomer from the gas phase: a) R-HDO (black) and S-HDO (red) over (+)-**1** (20 cycles) and b) R-HDO (black) and S-HDO (red) over (−)-**1** (20 cycles). The difference in the absolute adsorption values for the two samples may arise from a slight difference in the total amount of SURMOF deposited on the QCM substrate surface.

In summary, enantiopure MOF thin films have grown with control of orientation in (110) and (001) direction on MHDA and PPMT SAMs, respectively, and were characterized by both out-of-plane and in-plane surface X-ray diffraction. The enantiomeric SURMOFs $[\{Zn_2((+)cam)_2(dabco)\}_n]$ ((+)-**1**) and $[Zn_2((-)cam)_2(dabco)\}_n]$ (−-**1**) were fabricated directly on the SAM/Au modified QCM substrate and these samples enable the adsorption kinetics of enantiomers to be monitored and characterized. The difference of absolute uptake and absorption rate for each of the chosen enantiomeric probe molecules (2*R*,5*R*)-2,5-hexanediol (R-HDO) and (2*S*,5*S*)-2,5-hexanediol (S-HDO) is clear, and show significant enantioselectivity. Because QCM cannot distinguish R- from S-HDO by the mass uptake only, data on racemate separation cannot be gained using this approach. However, a stepwise LBL-like coating of the inner walls of SAM-functionalized fused silica GC-capillaries with enantiopure MOF thin films is now a straight forward task, as was recently shown for achiral MOF-5 coatings.[14] The respective enantiopure (SUR)MOF coatings are likely to show excellent performance as stationary phases to separate racemates by GC. The SURMOFs grown on QCM substrates as described herein may serve as valuable devices for (high throughput) automatic screening MOFs and analytes to optimize enantioselectivity in chiral separations.

Experimental Section

Preparation of (+)-**1**: The PPMT (PPMT = (4,(4-pyridyl)phenyl)methanethiol) and MHDA (MHDA = 16-mercaptohexadecanoic acid)

SAMs were fabricated following standard procedures using either 150 nm Au/2 nm Ti evaporated on Si wafers, or commercially available quartz crystal microbalance (QCM) Au substrates. The components were applied as diluted ethanol solutions: Zn^{II} acetate hydrate (0.5 mM), an equimolar (+)camH_2/dabco mixture (0.2 mM) Typical experiments were carried out using the automated QCM instrument Q-Sense E4 Auto at 40 °C and at flow rates of 100 μL min^{-1}. Each experiment started by exposing the substrates to the Zn^{II} acetate solution for 5 min and then a mixture of linker (+)camH_2/dabco for 10 min. Each subsequent step of dosing components was separated by a washing step of 5 min with pure ethanol. The enantiomeric SURMOF of (−)-**1** was prepared accordingly. A total of 20–40 growth cycles were carried out in each of the experiments.

Adsorption of the enantiomer by gas-phase QCM: Typically, 20 growth cycles for SURMOF (+)-**1** fabricated on MHDA SAM on QCM gold substrate were applied. The SURMOF sample was treated by vacuum to remove the ethanol molecules (solvent) hosted in MOFs. Before switching to the vessel containing R-HDO or S-HDO, pure nitrogen gas (carrier gas) was passed over the SURMOF sample to obtain a stable baseline. The adsorption curve was recorded by QCM. The adsorption experiments are performed at room temperature and a flow rate of 100 sccm controlled by a flow meter.

Received: June 20, 2011
Revised: July 27, 2011
Published online: November 3, 2011

Keywords: enantioselective adsorption · enantiopure metal–organic frameworks · quartz crystal microbalance · surface chemistry · thin films

[1] a) G. Férey, *Chem. Soc. Rev.* **2008**, *37*, 191 – 214; b) For a selection of current Reviews see themed issue on "Metal – Organic Frameworks" (Eds.: J. Long, O. Yaghi, *Chem. Soc. Rev.* **2009**, *38*, 1203 – 1504); c) For a cross-section of hot-topics see the recent issue on "Targeted Fabrication of MOFs for Hybrid Functionality", *Eur. J. Inorg. Chem*, **2010**, *24*, 3683 – 3874.

[2] a) D. Zacher, R. Schmid, C. Wöll, R. A. Fischer, *Angew. Chem.* **2011**, *123*, 184 – 208; *Angew. Chem. Int. Ed.* **2011**, *50*, 176 – 199; b) O. Shekhah, J. Liu, R. A. Fischer, C. Wöll, *Chem. Soc. Rev.* **2011**, *40*, 1081 – 1106.

[3] O. Shekhah, H. Wang, S. Kowarik, F. Schreiber, M. Paulus, M. Tolan, C. Sternemann, F. Evers, D. Zacher, R. A. Fischer, C. Wöll, *J. Am. Chem. Soc.* **2007**, *129*, 15118 – 15119.

[4] a) O. Shekhah, H. Wang, D. Zacher, R. A. Fischer, C. Wöll, *Angew. Chem.* **2009**, *121*, 5138 – 5142; *Angew. Chem. Int. Ed.* **2009**, *48*, 5038 – 5041; b) R. Makiura, S. Motoyama, Y. Umemura, H. Yamanaka, O. Sakata, H. Kitagawa, *Nat. Mater.* **2010**, *9*, 565 – 571.

[5] a) M. D. Allendorf, R. J. T. Houk, L. Andruszkiewicz, A. A. Talin, J. Pikarsky, A. Choudhury, K. A. Gall, P. J. Hesketh, *J. Am. Chem. Soc.* **2008**, *130*, 14404 – 14405; b) L. E. Kreno, J. T. Hupp, R. P. Van Duyne, *Anal. Chem.* **2010**, *82*, 8042 – 8046.

[6] a) D. Zacher, K. Yusenko, A. Bétard, K. Henke, M. Molon, L. Ladnorg, O. Shekhah, B. Schüpbach, T. de Los Arcos, M. Meilikhov, A. Terfort, C. Wöll, R. A. Fischer, *Chem. Eur. J.* **2011**, *17*, 1448 – 1455; b) O. Shekhah, K. Hirai, H. Wang, H. Uehara, M. Kondo, S. Diring, D. Zacher, R. A. Fischer, O. Sakata, S. Kitagawa, S. Furukawa, C. Wöll, *Dalton Trans.* **2011**, *40*, 4954 – 4958; c) K. Yusenko, M. Meilikhov, D. Zacher, F. Wieland, C. Sternemann, Xia. Stammer, T. Ladnorg, C. Wöll, R. A. Fischer, *CrystEngComm* **2010**, *12*, 2086 – 2090.

[7] O. Shekhah, H. Wang, M. Paradinas, C. Ocal, B. Schüpbach, A. Terfort, D. Zacher, R. A. Fischer, C. Wöll, *Nat. Mater.* **2009**, *8*, 481 – 484.

[8] B. Liu, M. Ma, D. Zacher, A. Betard, K. Yusenko, N. Metzler-Nolte, C. Wöll, R. A. Fischer, *J. Am. Chem. Soc.* **2011**, *133*, 1734 – 1737.

[9] O. Zybaylo, O. Shekhah, H. Wang, M, Tafipolsky, R. Schmid, D. Johannsmann, C. Wöll, *Phys. Chem. Chem. Phys.* **2010**, *12*, 8092 – 8097.

[10] a) L. Alaerts, M. Maes, L. Giebeler, P. A. Jacobs, J. A. Martens, J. F. M. Denayer, C. E. A. Kirschhock, D. E. De Vos, *J. Am. Chem. Soc.* **2008**, *130*, 14170 – 14178; b) S. Takamizawa, Y. Takasaki, R. Miyake, *J. Am. Chem. Soc.* **2010**, *132*, 2862 – 2863; c) H.-L. Jiang, Y. Tatsu, Z.-H. Lu, Q. Xu, *J. Am. Chem. Soc.* **2010**, *132*, 5586 – 5587.

[11] S. Han, Y. Wei, C. Valente, I. Lagzi, J. J. Gassensmith, A. Coskun, J. F. Stoddart, B. A. Grzybowski, *J. Am. Chem. Soc.* **2010**, *132*, 16358 – 16361.

[12] a) A. I. Skoulidas, *J. Am. Chem. Soc.* **2004**, *126*, 1356 – 1357; b) A. I. Skoulidas, D. S. Sholl, *J. Phys. Chem. B* **2005**, *109*, 15760 – 15768; c) L. Sarkisov, T. Düren, R. Q. Snurr, *Mol. Phys.* **2004**, *102*, 211 – 221.

[13] F. Stallmach, S. Groger, V. Kunzel, J. Karger, O. M. Yaghi, M. Hesse, U. Muller, *Angew. Chem.* **2006**, *118*, 2177 – 2181; *Angew. Chem. Int. Ed.* **2006**, *45*, 2123 – 2126.

[14] A. S. Münch, J. Seidel, A. Obst, E. Weber, F. O. R. L. Mertens, *Chem. Eur. J.* **2011**, *17*, 10958 – 10964.

[15] a) D. N. Dybtsev, H. Chun, K. Kim, *Angew. Chem.* **2004**, *116*, 5143 – 5146; *Angew. Chem. Int. Ed.* **2004**, *43*, 5033 – 5036; b) H. Chun, D. N. Dybtsev, H. Kim, K. Kim, *Chem. Eur. J.* **2005**, *11*, 3521 – 3529; c) D. Tanaka, M. Higuchi, K. Hasegawa, S. Horike, R. Matsuda, Y. Kinoshita, N. Yanai, S. Kitagawa, *Chem. Asian J.* **2008**, *3*, 1343 – 1349; d) T. Uemura, Y. Ono, K. Kitagawa, S. Kitagawa, *Macromolecules* **2008**, *41*, 87 – 94.

[16] D. N. Dybtsev, M. P. Yutkin, E. V. Peresypkina, A. V. Virovets, C Serre, G. Férey, V. P. Fedin, *Inorg. Chem.* **2007**, *46*, 6843 – 6845.

[17] a) J. Aizenberg, A. J. Black, G. M. Whitesides, *J. Am. Chem. Soc.* **1999**, *121*, 4500 – 4509; b) J. Aizenberg, A. J. Black, G. M. Whitesides, *Nature* **1999**, *398*, 495 – 498; c) D. Qin, Y. N. Xia, B. Xu, H. Yang, C. Zhu, G. M. Whitesides, *Adv. Mater.* **1999**, *11*, 1433 – 1437.

[18] R. Vaidhyanathan, D. Bradshaw, J. Rebilly, J. P. Barrio, J. A. Gould, N. G. Berry, M. J. Rosseinsky, *Angew. Chem.* **2006**, *118*, 6645 – 6649; *Angew. Chem. Int. Ed.* **2006**, *45*, 6495 – 9499.

